Polymeric micelle mediated follicular delivery of spironolactone: Targeting the mineralocorticoid receptor to prevent glucocorticoid-induced activation and delayed cutaneous wound healing

Naoual Dahmana, Thibault Mugnier, Doris Gabriel, Tatiana Favez, Laura Kowalczuk, Francine Behar-Cohen, Robert Gurny, Yogeshvar N Kalia

Journal Pre-proofs

Polymeric micelle mediated follicular delivery of spironolactone: Targeting the mineralocorticoid receptor to prevent glucocorticoid-induced activation and delayed cutaneous wound healing

Naoual Dahmana, Thibault Mugnier, Doris Gabriel, Tatiana Favez, Laura Kowalczuk, Francine Behar-Cohen, Robert Gurny, Yogeshvar N. Kalia

PII: S0378-5173(21)00578-0
DOI: https://doi.org/10.1016/j.ijpharm.2021.120773
Reference: IJP 120773

To appear in: *International Journal of Pharmaceutics*

Received Date: 30 March 2021
Revised Date: 31 May 2021
Accepted Date: 2 June 2021

Please cite this article as: N. Dahmana, T. Mugnier, D. Gabriel, T. Favez, L. Kowalczuk, F. Behar-Cohen, R. Gurny, Y.N. Kalia, Polymeric micelle mediated follicular delivery of spironolactone: Targeting the mineralocorticoid receptor to prevent glucocorticoid-induced activation and delayed cutaneous wound healing, *International Journal of Pharmaceutics* (2021), doi: https://doi.org/10.1016/j.ijpharm.2021.120773

Polymeric micelle mediated follicular delivery of spironolactone: Targeting the mineralocorticoid receptor to prevent glucocorticoid-induced activation and delayed cutaneous wound healing

Naoual Dahmana[a,b], Thibault Mugnier[c], Doris Gabriel[c], Tatiana Favez[d], Laura Kowalczuk[d], Francine Behar-Cohen[d,e], Robert Gurny[a,b,c], Yogeshvar N. Kalia[a,b] *

CRediT authorship contribution statement

Naoual Dahmana: Conceptualization; Data curation; Investigation; Methodology; Visualization; Writing - original draft.

Thibault Mugnier: Investigation; Methodology.

Doris Gabriel: Investigation; Methodology; Conceptualization.

Tatiana Favez : Investigation; Methodology.

Laura Kowalczuk: Investigation; Methodology; Conceptualization; Writing - review & editing.

Francine Behar-Cohen: Conceptualization; Funding acquisition; Project administration; Resources; Writing - review & editing

Robert Gurny: Conceptualization; Funding acquisition; Project administration; Resources; Supervision, Writing - review & editing

Yogeshvar N. Kalia: Conceptualization; Data curation; Formal analysis; Funding acquisition; Project administration; Resources; Supervision; Writing - review & editing.

[a] School of Pharmaceutical Sciences, University of Geneva, CMU - 1 rue Michel Servet, 1211 Geneva 4, Switzerland.

[b] Institute of Pharmaceutical Sciences of Western Switzerland, University of Geneva, CMU - 1 rue Michel Servet, 1211 Geneva 4, Switzerland.

[c] Apidel SA, 29 Quai du Mont Blanc, 1201 Geneva, Switzerland.

[d] Fondation Asile des Aveugles - Hôpital Ophtalmique Jules-Gonin, 15 Avenue de France, 1004 Lausanne, Switzerland.

[e] INSERM, UMRS 872 Team 17, Centre de Recherche des Cordeliers, 15 rue de l'Ecole de Médecine, 75006 Paris, France.

*Corresponding author:

School of Pharmaceutical Sciences
University of Geneva
CMU – 1 rue Michel Servet
1211 Geneva 4
Switzerland

Yogi.Kalia@unige.ch, Tel.: +41 22 379 3355; fax: +41 22 379 3360.

Electronic supplementary information (ESI) available.

ABSTRACT

Impaired wound healing in patients receiving glucocorticoid therapy is a serious clinical concern: mineralocorticoid receptor (MR) antagonists can counter glucocorticoid-induced off-target activation of MR receptors. The aim of this study was to investigate the cutaneous delivery of the potent MR antagonist, spironolactone (SPL), from polymeric micelle nanocarriers, prepared using a biodegradable copolymer, methoxy-poly(ethylene glycol)-di-hexyl-substituted-poly(lactic acid). Immunofluorescent labelling of the MR showed that it was principally located in the pilosebaceous unit (PSU), justifying the study rationale since polymeric micelles accumulate preferentially in appendageal structures. Cutaneous biodistribution studies under infinite and finite dose conditions, demonstrated delivery of pharmacologically relevant amounts of SPL to the epidermis and upper dermis. Preferential PSU targeting was confirmed by comparing amounts of SPL in PSU-containing and PSU-free skin biopsies: SPL nanomicelles showed 5-fold higher delivery of SPL in the PSU-containing biopsies, 0.54±0.18 ng/mm^2 vs. 0.10±0.03 ng/mm^2, after application of a hydrogel in finite conditions. Canrenone, an active metabolite of SPL, was also quantified in skin samples. In addition to being used for the treatment of delayed cutaneous wound healing by site-specific antagonism of the MR, the formulation might also be used to treat pilosebaceous androgen-related skin diseases, e.g. acne vulgaris, since SPL is a potent androgen receptor antagonist.

Keywords: spironolactone; micelles; methoxy-poly(ethylene glycol)-di-hexyl-substituted-poly(lactic acid); follicular delivery; cutaneous biodistribution; mineralocorticoid receptor; immunofluorescence; wound healing; acne; androgen receptor antagonist.

1. Introduction

Impaired cutaneous wound healing is a significant clinical problem encountered as a complication of certain chronic conditions such as diabetes as well as in patients under chronic glucocorticoid therapy (Werner and Grose, 2003). Recent studies have elucidated the mechanism involved in glucocorticoid-induced delayed wound healing and have attributed it to off-target over-activation of the mineralocorticoid receptor (MR) by glucocorticoids (Boix et al., 2016; Farman et al., 2010; Schacke et al., 2002).

Based on this observation, co-administration of a MR antagonist with a glucocorticoid was suggested as a therapeutic strategy to block off-target glucocorticoid binding to the MR. This hypothesis was tested *in vivo* in mice where wounds treated topically with clobetasol, a potent glucocorticoid and canrenoate potassium, a water-soluble precursor of canrenone (an active metabolite of the potent MR antagonist, spironolactone (SPL; MW 416.57 g/mol, log P 2.78)), indicated for intravenous administration, showed a significant improvement in wound closure compared to the control (clobetasol + PBS) (Nguyen et al., 2016). Moreover, a clinical trial conducted in 23 healthy volunteers showed a significant off-setting of clobetasol-induced skin atrophy upon co-administration of spironolactone – however, the formulation contained a 100-fold excess of SPL (5% vs 0.05% clobetasol) (Maubec et al., 2015). Given the positive results seen after the co-administration of MR antagonists and the potential clinical benefits for patients under glucocorticoid therapy and suffering from wound healing abnormalities, it was decided to develop a more rational spironolactone formulation for topical application to the skin and so address the unmet clinical need.

Spironolactone is a potent MR antagonist but it is poorly water-soluble (0.02 mg/mL) making its formulation in a patient-friendly formulation a challenge. To enhance the aqueous solubility of SPL, we decided to use the micelle forming amphiphilic copolymer; methoxy-poly(ethylene glycol)-di-hexyl-substituted-poly(lactic acid), (mPEG-hexPLA), which was able to increase aqueous solubility by ~100-fold yielding a micellar solution of SPL with concentration of ~2 mg/mL. This biodegradable and biocompatible diblock copolymer has already shown its utility for the topical delivery of poorly water-soluble compounds by enhancing their bioavailability in the skin and the cornea (Dahmana et al., 2018b; Di Tommaso et al., 2012; Gabriel et al., 2016; Lapteva et al., 2015; Lapteva et al., 2014a; Lapteva et al., 2014b).

We have previously developed and characterized a 0.1% SPL nanomicellar solution based on mPEG-dihexPLA copolymer that showed a stability of at least 12 months at 5°C. The preclinical tolerability and efficacy of this formulation was assessed *in vivo* in rabbits in a corneal wound healing model where co-administration of this formulation offset dexamethasone-induced corneal delayed wound healing (Dahmana et al., 2018b).

There is no commercially available topical formulation of SPL. As a result, oral SPL is being increasingly used off-label to treat dermatological conditions, e.g. acne vulgaris, androgenic alopecia and hirsutism, as it is a potent androgenic antagonist. However, given its affinity for the MR and ability to bind to other steroid receptors, oral administration of SPL to treat localized diseases is undesirable since systemic exposure clearly increases the risk of undesirable side effects (Afzali et al., 2012a; Brown et al., 2009; Kelidari et al., 2016).

The first part of the present study involved the use of immunofluorescent labelling to investigate the distribution of the MR in porcine skin: Kenouch *et al*., had reported the presence of the MR in human epidermis and appendages and the objective here was to confirm that this was also the case for porcine skin (Farman et al., 2010; Jaisser and Farman, 2016; Kenouch et al., 1994). These studies revealed that MR were principally present in the pilosebaceous unit (PSU). Recent investigations have shown a preferential accumulation of nano-sized polymeric micelles in the PSU, resulting in a topical, efficient treatment for diseases involving the hair follicle and the sebaceous glands such as acne vulgaris (Kandekar et al., 2017; Lapteva et al., 2015). Hence, developing a novel nanomicellar drug delivery system for topical delivery of SPL would allow site-specific targeting of the MR with potential for greater efficacy and reduced off-site side effects. For a more patient-friendly dermatologic administration, the SPL nanomicellar solution was incorporated in a Carbopol® based hydrogel and skin penetration *in vitro* was evaluated following topical application under both infinite and finite dose conditions (as specified in the OECD Guidelines) (OECD, 2004). The safety of the composite nanomicellar hydrogels based on Carbopol® and mPEG-hexPLA had already been tested and no signs of toxicity were observed following multiple topical application in healthy mice (Gabriel et al., 2016). Following formulation development, the cutaneous biodistribution of SPL and its two main active metabolites, 7α-thiomethylspironolactone and canrenone, was determined by quantifying the amount of each substance as a function of skin depth using a validated UHPLC-ESI-MS analytical method (Dahmana et al., 2018a). Follicular delivery of SPL nanomicelles was investigated by quantifying the amounts present in PSU-containing and PSU-free skin biopsies – in addition to quantification of the absolute amounts present, the delivery efficiencies of the 0.1% SPL nanomicellar solution and hydrogel were also compared.

2. Materials and Methods

2.1. Materials

Methoxy-poly(ethylene glycol)-di-hexyl-substituted-poly(lactic acid) (Trimaille et al., 2006), (mPEG-dihexPLA, 5.5 kDa) was supplied by Apidel SA (Geneva, Switzerland). Spironolactone (SPL) was purchased from Zhejiang Langhua pharmaceutical Co., Ltd. (Zhejiang, China). 7α-thiomethylspironolactone (TMSPL) was purchased from TLC Pharmaceutical Standards Ltd. (Ontario, Canada). Canrenone (CAN) and 17α-methyltestosterone (MeT), used as an internal standard (IS), were purchased from Sigma-Aldrich (Buchs, Switzerland). Carbopol® Ultrez 10 was obtained from Lubrizol (Belgium). Millex® filters (Durapore PVDF, pore size 0.22 µm, diameter 13 mm) were purchased from Sigma-Aldrich (Buchs, Switzerland). Ultrapure water (H_2O, resistivity > 18 MΩ cm) was prepared using a Merck Millipore Milli-Q water purification system (Darmstadt, Germany). Methanol (MeOH, HPLC grade) was obtained from Fisher Scientific (Waltham, MA, USA) and formic acid (ULC/MS grade) from Biosolve (Dieuze, France). Trifluoroacetic acid was obtained from VWR (Dietikon, Switzerland). All other chemicals were at least of analytical grade. MR antibody (MABS496) and DAPI were obtained from Merck Millipore (Darmstadt, Germany).

2.2. Analytical methods

2.2.1. Quantification of spironolactone in the formulations using UHPLC-UV

An ultra-high performance liquid chromatography method with UV detection (UHPLC-UV) was developed to support the formulation development work. The liquid chromatographic system consisted of a Waters Acquity® UPLC® H-Class system (Baden-Dättwil, Switzerland) including a binary solvent manager, a sample manager and a column manager. Reverse phase chromatography was performed using a Waters XBridge® BEH C18 column (50 x 2.1 mm I.D., 2.5 µm) fitted with a Waters XBridge® BEH C18 VanGuard pre-column (5 x 2.1 mm I.D., 2.5 µm). Isocratic elution was carried out using a mobile phase consisting of 0.1% formic acid in H_2O:MeOH (30:70, v/v) with a flow rate of 0.45 mL/min and a runtime of 1 min. Column temperature was held at 40°C and the sample manager was kept at room temperature. Injection volume was 10 µL and the UV detection of SPL was set at 240 nm. Calibration standards of SPL were prepared in methanol:water (1:1) mixture at 0.1, 0.2, 0.5, 1, 2, 5, and 10 µg/mL. Calibration curves were constructed by plotting the area of each analyte against the concentration of each analyte. All the calibration curves were linear (R > 0.99). The limit of detection (LOD) and the limit of quantification (LOQ) of SPL were 0.1 µg/mL and 0.2 µg/mL, respectively. More information is provided in the **ESI** (**Fig S1** and **Table S1**).

2.2.2. Quantification of spironolactone and its metabolites in the skin using UHPLC-ESI-MS

A published bioanalytical method involving ultra-high performance liquid chromatography coupled to mass spectrometry (UHPLC-ESI-MS) for the simultaneous detection and quantification of spironolactone (SPL) and its metabolites, 7α-thiomethylspironolactone (TMSPL) and canrenone (CAN), in ocular tissue, with 17α-methyltestosterone (MeT) as internal standard, was adapted and validated for used with skin samples (see ESI) (Dahmana et al., 2018a). This sensitive method was specifically developed to allow precise separation and quantification of SPL and its metabolites in small samples such is in the different tissues of the ocular globe or in the different layers of the skin. Briefly, the liquid chromatographic system consisted of a Waters Acquity® ultra-performance liquid chromatography (UPLC®) system (Baden-Dättwil, Switzerland) including a binary solvent manager, a sample manager with an injection loop volume of 10 µL and a column manager. Reverse phase chromatographic separation of SPL, TMSPL, CAN and MeT was performed using a Waters XBridge® BEH C18 column (100 x 2.1 mm I.D., 2.5 µm) fitted with a Waters XBridge® BEH C18 VanGuard pre-column (5 x 2.1 mm I.D., 2.5 µm). Isocratic elution was carried out using a mobile phase consisting of 0.1% formic acid in H_2O:MeOH (50:50, v/v) with a flow rate of 0.3 mL/min and a runtime of 12 minutes. Column temperature was held at 50°C and the sample manager was kept at room temperature. Injection volume was set at 5 µL (partial loop injection mode). The mass spectrometry (MS) system consisted of a Waters XEVO® TQ-MS detector (Baden-Dättwil, Switzerland) fitted with a Z-spray electrospray ionization source. MS detection of the 4 compounds was performed using electrospray ionization in the positive-ion mode (ESI+) and the selected ion recording (SIR) using the pseudo-molecular ion of each compound as the parent ion (hydrogen adduct, $[M + H]^+$). The capillary voltage was set at 2.3 kV, and desolvation gas temperature and flow were maintained at 350 °C and 650 L/h, respectively. Identification and quantification of each analyte were carried on according to the mass-to-charge ratio (m/z) of the pseudo-molecular ion of each compound ($[M + H]^+$). Cone voltage optimal setting was 35 V and the pseudo-molecular parent ion corresponding to SPL/CAN, TMSPL and MeT have an *m/z* of 341.0, 389.0 and 303.0 respectively. SPL was detected with *m/z* of 341.0, which corresponds to the pseudo-molecular parent ion of CAN. This is due to the cleavage of the 7α-thioacetyl group of SPL during the electrospray evaporation and ionization process within the ESI source producing CAN. Dwell time was set at 5 ms for all the compounds. Data processing was performed using Waters MassLynx software version 4.1 (Milford, MA, USA). Calibration standards of SPL, TMSPL and CAN were prepared in porcine skin matrix at 5, 10, 20, 50, 200, 500 and 1000 ng/mL, and contained 100 ng/mL 17α-methyltestosterone as internal standard (IS). Calibration curves were constructed by plotting the ratio of the area of each analyte to the area of the internal standard *versus* the ratio of the concentration of each analyte to the concentration of the internal standard. All calibration curves were linear (R > 0.99). The lower limit of quantification (LLOQ) of each analyte was 5 ng/mL. Complete information is provided in the **ESI** (**Figs S2-S6** and **Table S2**).

2.3. Mineralocorticoid receptor labelling in the skin

The localization of the MR in the skin was determined using immunofluorescent labelling. Skin biopsies were punched from the external part of fresh porcine ears obtained from a local slaughterhouse (CARRE; Rolle, Switzerland) then fixed in 4 mL of 4% paraformaldehyde in PBS for 1 h at room temperature followed by rinsing three times in PBS. Samples were cryoprotected using sucrose gradient solutions (10% then 20%) during 2 h at room temperature and finally left overnight in 30% sucrose solution at 5°C. The following day, the samples were cryoembedded in OCT compound at -40°C for 45 s using the PrestoCHILL device (Milestone, Italy), cut into 5 µm serial sections (CryoStar NX70 Cryostat, Thermo Scientific) and then mounted on glass slides and kept at -20°C until analysis. Prior to immunofluorescent labelling, skin sections were fixed using methanol for 10 min at -20°C then rinsed three times with PBS. Nonspecific protein binding was blocked using a blocking solution containing 5% Normal Goat Serum (NGS) and 0.3% Triton-X-100 in PBS for 1 h at 5°C then skin sections were incubated overnight at 5°C with the MR primary antibody diluted 1:100 in 1% Bovine Serum Albumin (BSA) and 0.3% Triton-X-100 in PBS. After three rinsing cycles with PBS, skin sections were incubated with the secondary antibody (Goat Anti-Mouse Alexa 488) diluted 1:2000 in 1% BSA and 0.3% Triton-X-100 in PBS for 1 h at room temperature, away from light, then rinsed three times in PBS. DAPI was used as nuclear counterstain. Skin sections were incubated with DAPI (stock solution diluted 1:1000 in PBS) during 5 min at room temperature followed by 3 rinsing cycles in PBS. Finally, skin samples were mounted using a mounting medium (Mowiol®) and a cover slip then left to dry overnight at room temperature and away from light. Glass slides were stored at -20°C until imaging. Throughout the experiment, glass slides were placed in a humid plate to prevent dryness and covered with foil when incubated with secondary antibody.

2.4. Confocal microscopy settings

Imaging of the immunolabelled skin sections was performed using a Leica SP8 confocal laser scanning microscope (CLSM - Leica, Germany) equipped with a HC PL APO CS2 20×/0.75 immersion objective (Leica, Germany). Microscope settings are summarized in **Table 1**.

Table 1
Settings used for confocal microscopy.

Dye	Laser Type	λ Excitation	Laser Intensity	λ Emission	Detector	Gain	Pinhole
DAPI	Diode	405 nm	3.5%	480 nm	PMT (411-474 nm)	771	46.9 µm
Alexa 488	Diode	488 nm	9.7%	520 nm	HyD (493-557 nm)	100	50.8 µm

2.5. Spironolactone nanomicellar formulations

A concentrated SPL nanomicellar solution was prepared at 2 mg/mL using mPEG-hexPLA copolymer. Briefly, 10 mg SPL and 400 mg mPEG-hexPLA were dissolved in 1.5 mL acetone. Subsequently, this solution was added dropwise using a syringe pump (6 mL/h) to 5 mL of the aqueous phase – consisting of citrate buffer (20 mM, pH 5.5) – under sonication (20 % amplitude, S 450 D, Branson, USA), then acetone was removed under reduced pressure (58°C, 180 mbar). Finally, the formulation was filtered through 0.22 µm PVDF filter into a sterilized vial and kept at 5°C.

In parallel, a concentrated 1.6% (w/w) Carbopol® based hydrogel was prepared by dissolving 160 mg Carbopol® Ultrez 10 in 8 g MilliQ water, containing 4 mg benzalkonium chloride as a preservative. The pH was adjusted to 5.6 by dropwise addition of NaOH (10% solution) under magnetic stirring then the weight was adjusted to 10 g with MilliQ water.

Finally, 0.1% (w/v) SPL nanomicellar solution and hydrogel were obtained by 1:1 (w/w) dilution of the 0.2% (w/v) spironolactone nanomicellar solution with MilliQ water and 1.6% (w/w) Carbopol® hydrogel, respectively. Briefly, 3 g of 0.2% (w/v) spironolactone nanomicellar solution were weighed in a beaker and were added to 3 g of either MilliQ water or 1.6% (w/w) Carbopol® hydrogel, then the mix was homogenized by gentle stirring using a magnetic bar to yield a final 0.1% (w/v) SPL nanomicellar solution or hydrogel (0.8% (w/w) Carbopol®) (**Table 2)**. Finally, formulations were characterized in terms of micelle size, pH and viscosity. Spironolactone content was quantified by HPLC-UV. Drug loading and incorporation efficiency were calculated using the following equations:

$$\text{Drug Loading(mg/g)} = \frac{\text{Mass of drug incorporated in micelles (mg)}}{\text{Mass of copolymer used (g)}}$$

Eq. 1

$$\text{Incorporation Efficiency (\%)} = \frac{\text{Actual drug loading}}{\text{Target drug loading}} \text{ x } 100$$

Eq. 2

Table 2
Composition of the different spironolactone nanomicellar formulations.

Formulation	[SPL]	[Citrate Buffer]	[mPEG-dihexPLA]	[Carbopol® Ultrez 10]
0.2% SPL nanomicellar solution	2 mg/mL	20 mM	80 mg/mL	-
0.1% SPL nanomicellar solution	1 mg/mL	10 mM	40 mg/mL	-
0.1% SPL nanomicellar hydrogel	1 mg/mL	10 mM	40 mg/mL	0.8%

2.6. Viscosity measurement

Viscosity was measured using the Haake® Mars® 40 rheometer fitted with a cone-plate measuring geometry (sensor C35/2° Ti – 35 mm diameter, cone-plate angle of 2°). Rheological measurements and data processing were performed with the RheoWin software. 400 µL hydrogel was deposited in the middle of the plate then the measurement was set in the rotary mode, with a shear rate of 4.3 s^{-1} over 30 s at 20 °C.

2.7. Size determination

The number weighted (d_n) and intensity weighted (Z-average, Z_{av}) hydrodynamic diameters and the polydispersity index (PDI) of the SPL micelles were measured using a Zetasizer Nano-ZS (Malvern Instruments, UK). SPL nanomicellar solutions were diluted and homogenized in MilliQ water to a final copolymer concentration of 20 mg/mL (1:1 for 0.1% concentration and 1:3 for the 0.2% concentration) then filled into disposable plastic cuvettes for analysis with back scattering light (173 degrees). Samples were equilibrated at 25°C before the first measurement.

2.8. Morphology visualization

Micelles were visualized using transmission electron microscope (TEM, FEI Tecnai™ G2 Sphera, Oregon, USA). Briefly, the 0.1% nanomicellar solution was diluted 1:10 in MilliQ water, then 5 µL were deposited on a grid, left for 30 s and the excess was carefully wiped. Subsequently, one drop of 2% uranyl acetate was applied during 30 s to enhance the contrast and the excess was carefully removed. TEM magnification was set at 25000x.

2.9. *In vitro* skin delivery experiments

These were performed using Franz diffusion cells to evaluate the deposition in and transdermal permeation across porcine skin of SPL following topical application of the 0.1% spironolactone nanomicellar formulations. All the experiments were performed according to the OECD guidelines (OECD, 2004).

2.9.1. Determination of spironolactone skin deposition and cutaneous biodistribution following topical application

Fresh porcine ears were obtained from a local slaughterhouse (CARRE; Rolle, Switzerland). After cleaning under running water, excess hair was clipped and the full thickness skin was harvested from the external part of the ear using a scalpel. Subsequently, skin biopsies were harvested using a 3.2 cm diameter punch and the underlying adipose tissue was excised using a Thomas Stadie-Riggs tissue slicer to yield skin disks with a final thickness of 1.0 ± 0.2 mm. Samples were stored at -20°C until use for a maximum period of 3 months.

Before use, skin samples were thawed and rehydrated in PBS (10 mM, pH 7.4) for 15 min then mounted on Franz cells and fixed with a clamp. Consequently, the donor compartment (2 cm^2 contact surface area) was filled with the 0.1% SPL nanomicellar formulation (solution, n=6 or hydrogel, n=6) and left unoccluded. The experiment was performed in both infinite dose (200 mg/cm^2) and finite dose (10 mg/cm^2) conditions. The receptor compartment was filled with 10 mL PBS (10 mM, pH 7.4) containing 1% BSA to ensure sink conditions. Franz cells were placed in a water bath maintained at 32 ± 1°C and the experiment was run for 12 h; 1 mL buffer aliquots were withdrawn from the receiver compartment, and replaced with fresh buffer at 2, 4, 8 and 12 h to quantify transdermal permeation.

At the end of the experiment, Franz cells were carefully dismantled and the skin samples rinsed under running water and carefully wiped with tissue (3 cycles). Subsequently, the treated area was punched out using a 1.6 cm diameter punch then samples were snap-frozen in isopentane cooled in liquid nitrogen. Samples were then cut into 40 µm thickness serial sections (CryoStar NX70 Cryostat, Thermo Scientific) from the skin surface to a depth of 400 µm; each section was placed in an Eppendorf tube containing 300 µL of the extraction solvent.

2.9.2. Investigation into preferential delivery of the spironolactone nanomicelles to the PSU

To evaluate the follicular delivery of SPL nanomicelles, another series of skin delivery experiments was performed as described above in which the deposition of SPL in skin samples containing the pilosebaceous unit (PSU-containing) was quantified and compared to control samples, without the PSU (PSU-free); the procedure has been described in detail in our earlier work (Kandekar et al., 2017; Lapteva et al., 2015). Briefly, porcine skin samples were prepared as described as above except that samples were kept at full thickness to preserve PSU integrity. Indeed, the hair follicle takes origin in the deepest dermis, sometimes even in the subcutaneous tissue with the hair bulb, then elongates through the dermis and the epidermis up to the skin surface with the hair shaft. Skin samples were placed in Franz cells then 0.1% SPL nanomicellar solution (n=6) or hydrogel (n=6) was applied to the skin under both infinite and finite dose conditions for each formulation. The experiment was run in the same conditions as above. After 12 h, the skin samples were cleaned as mentioned above and then skin biopsies containing the pilosebaceous unit (PSU, n=15) and control skin biopsies (PSU-free, n=15) were harvested using a 1 mm diameter punch and placed in Eppendorf tubes containing 100 µL of the extraction solvent.

2.9.3. Extraction procedure

Skin slices, PSU and PSU-free skin samples obtained from the deposition studies above were placed in Eppendorf tubes containing methanol:water (8:2) as extraction solvent and 100 ng/mL 17α-methyltestosterone as internal standard. The Eppendorf tubes were then placed in a shaking bath (150 min^{-1}) and left for extraction overnight at room temperature. The following day, samples were centrifuged (5000 rpm, 10 min) then the supernatant were quantified using the UHPLC-ESI-MS method. Validation of the extraction procedure is provided in the **ESI** (**Table S3**).

2.10. Statistical analysis

Statistics were calculated using SigmaPlot software. Results were statistically analysed using either *Student's t-test* or Mann-Whitney rank sum test. Data were expressed as the Mean ± SD. The level of significance was fixed at $\alpha=0.05$.

3. Results

3.1. Mineralocorticoid receptor labelling in the skin

The results of the immunofluorescent labelling studies confirmed the presence of the MR in porcine skin; it was shown to be mainly located in the skin appendages with a high predominance in the hair follicles and in the epithelial cells of the eccrine sweat glands (**Fig. 1**). The longitudinal sections of the hair follicles showed the presence of the MR in the hair bulb and in the inner and outer root sheaths. The outer root sheath is a stratified epithelium that is contiguous with the epidermis. Immunofluorescence was also detected in the epidermis and the dermis but with lower intensity compared to the hair follicle and sweat glands. In the dermis, the immunofluorescence signal may correspond to the MR localized in the endothelium of the vascular capillaries.

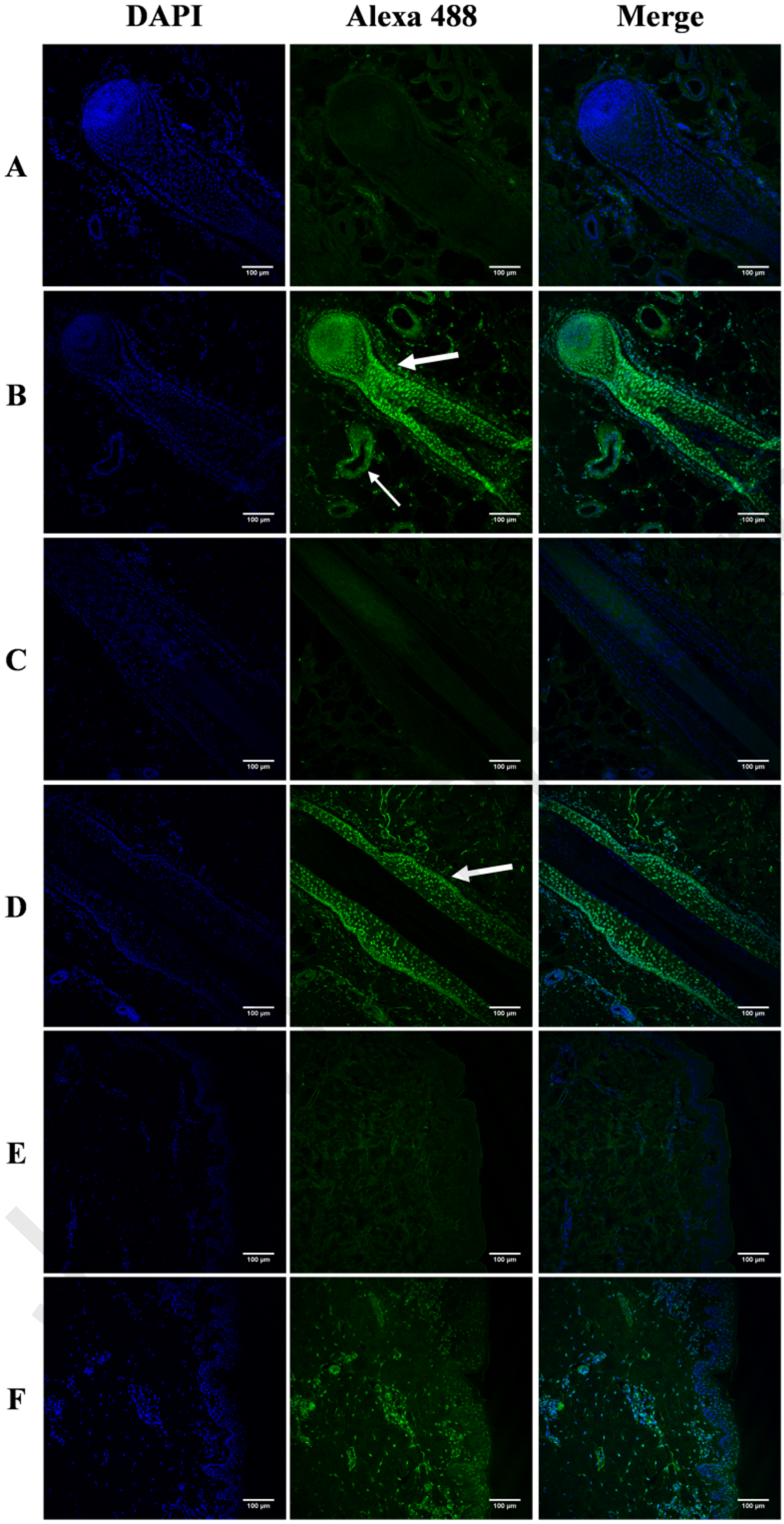

Fig. 1 Localization of the mineralocorticoid receptor in porcine skin. A and B, longitudinal sections of the hair follicle with the hair bulb located in the deeper dermis. C and D, longitudinal

sections of the hair follicle located in the mid-dermis. E and F, longitudinal sections of full thickness porcine skin. A, C and E, porcine skin incubated with Alexa 488 (control); B, D and F, porcine skin incubated with the MR antibody and Alexa 488. Thick arrows show the hair follicle, thin arrows show the eccrine sweat gland. Images obtained by CLSM (Leica SP8) under 20X objective lens. Scale bar 100 µm.

3.2. Spironolactone nanomicellar formulations

Spironolactone was efficiently encapsulated in the mPEG-hexPLA nanomicelles at 2.00 ± 0.11 mg/mL with 100.15 ± 0.11% incorporation efficiency. After 1:1 (w/w) dilution in MilliQ water, SPL concentration was 0.96 ± 0.03 mg/mL. Importantly, the size of the nanomicelles remained unchanged after dilution and was in the range of 20 nm (**Table 3**).

Table 3
Characteristics of the formulations prepared.

Formulation	[SPL] (mg/mL)	pH	Viscosity (Pa. s)	d_n (nm)	Z_{av} (nm)	PDI
0.2% SPL nanomicellar solution	2.00 ± 0.11	5.5	-	21	43	0.2
0.1% SPL nanomicellar solution	0.96 ± 0.03	5.7	-	21	43	0.2
0.1% SPL nanomicellar hydrogel	0.98 ± 0.01	5.6	20	21*	43*	-

***:** Extrapolated size of the nanomicelles from the solution to the hydrogel based on the integrity test performed using Nile Red-loaded nanomicelles (see ESI, Fig. S8).

TEM confirmed the spherical shape of the nanomicelles (**Fig. 2**).

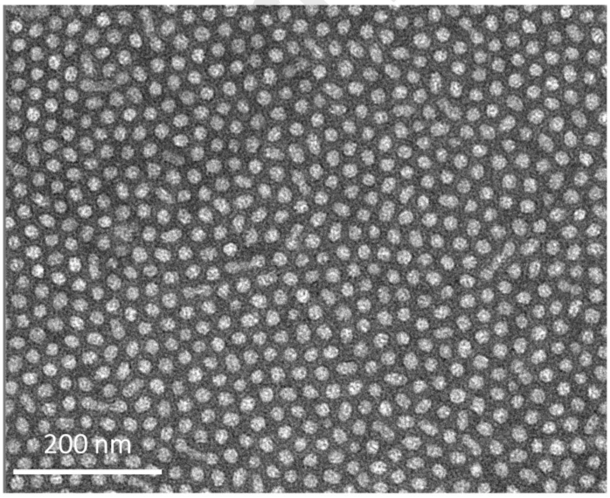

Fig. 2 Morphology of 0.1% spironolactone nanomicelles. Mean size of 20 nm.

Dilution of the 0.2% SPL nanomicellar solution 1:1 (w/w) in the concentrated 1.6% Carbopol® hydrogel resulted in the formation of a composite hydrogel with a final Carbopol® concentration of 0.8%. The unloaded hydrogel was transparent, SPL loaded nanomicellar solution and hydrogel were slightly turbid due to the colloidal suspension formed by the nanomicelles (see **ESI**, **Fig. S7**). The viscosity of the concentrated 1.6% Carbopol® hydrogel was 70 Pa.s, once diluted with the concentrated nanomicellar solution, the viscosity dropped to 20 Pa.s which is suitable for topical application. Indeed, the hydrogel was easily spreadable on the skin and evaporated quickly without leaving any sticky residue. The pH of the hydrogels remained identical before and after dilution and was 5.6 which is also optimal for skin application. The SPL concentration in the 0.1% SPL nanomicellar hydrogel was found to be 0.98 ± 0.01 mg/mL. The integrity of the SPL nanomicelles following mixing with the concentrated 1.6% Carbopol® hydrogel was assessed using Nile Red-loaded nanomicelles (see **ESI, Fig. S8**).

All the formulations were stable in terms of concentration, pH, viscosity and micelle size for at least 1 month at 5°C (see **ESI**, **Table S4**); the formulations' characteristics are summarized in **Table 3**.

3.3. Spironolactone skin deposition and biodistribution

Topical application of 0.1% SPL nanomicellar solution and hydrogel formulations for 12 h resulted in the deposition of therapeutic amounts of SPL in the epidermis and the upper dermis (to a depth of 400 μm) in both infinite and finite dose conditions (**Fig. 3**).

Qualitatively, the biodistribution profile was the same for both formulations regardless of the amount applied with a higher concentration at the surface of the skin and a gradual decrease in the amount delivered as a function of the skin depth (**Fig. 3**). However, in quantitative terms, there was a 10-fold decrease in the amount of SPL delivered to the skin after the 20-fold decrease in the amount of the formulation applied to the skin surface (200 mg/cm^2 *vs.* 10 mg/cm^2) upon going from infinite to finite dose conditions. Interestingly, topical application of 0.1% SPL nanomicellar formulations to porcine skin resulted in the formation of the metabolite canrenone; however, the other active metabolite, 7α-thiomethylspironolactone was not detected (**Fig. 3**).

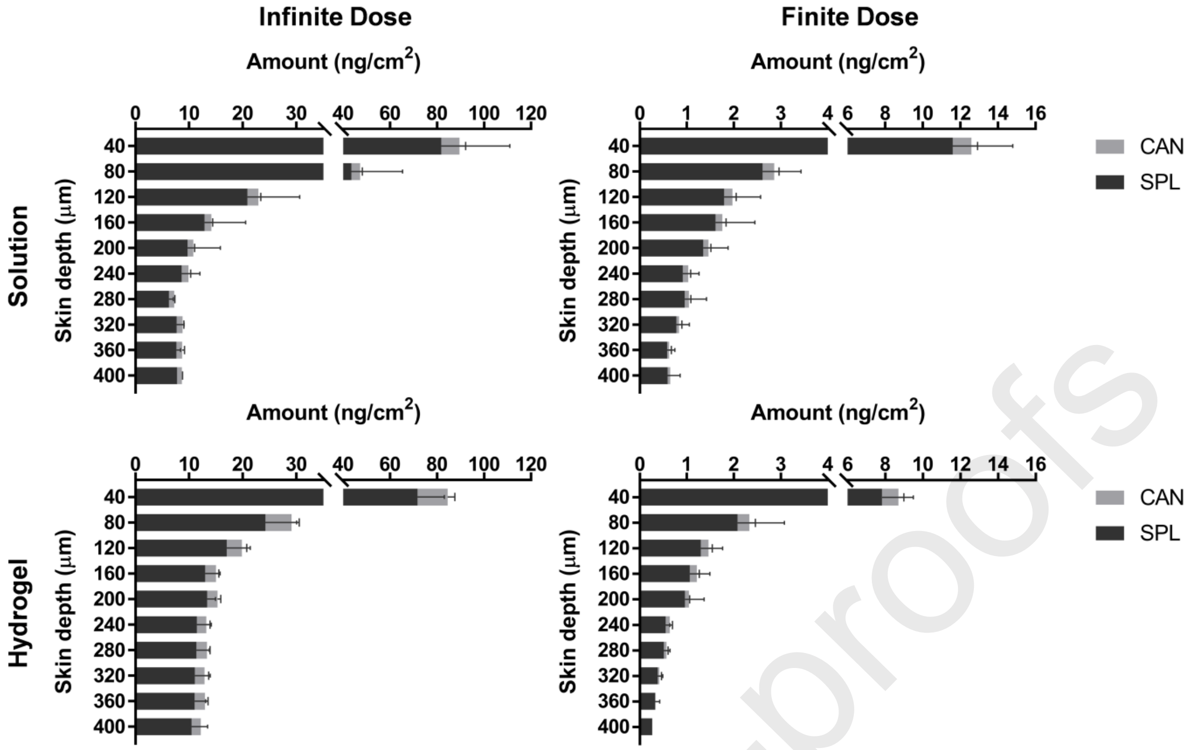

Fig. 3 Spironolactone and canrenone amounts in the epidermis and the upper dermis of porcine skin following topical application of 0.1% spironolactone nanomicellar solution and hydrogel in infinite and finite dose conditions. CAN, canrenone, SPL, spironolactone. Narrow head error bars, standard deviation of spironolactone amounts; large head error bars, standard deviation of canrenone amounts (Mean ± SD; n=6).

There were no statistically significant differences between the amounts of SPL delivered from the 0.1% SPL nanomicellar solution and hydrogel to the epidermis (up to 160 µm skin depth) following topical application under infinite (159.04 ± 57.77 and 125.86 ± 21.84 *vs.* ng/cm^2, respectively) and finite (17.62 ± 5.03 and 12.26 ± 3.22 *vs.* ng/cm^2, respectively) dose conditions. However, the hydrogel delivered significantly greater amounts than the solution to the upper dermis (160-400 µm skin depth), under infinite dose conditions (68.74 ± 13.02 *vs.* 47.68 ± 11.23 ng/cm^2, respectively; $p<0.001$, n=6). In contrast, the solution delivered significantly greater amounts of SPL to the upper dermis than the hydrogel under finite dose conditions (5.17 ± 1.81 *vs.* 3.01 ± 0.76 ng/cm^2, respectively; $p=0.042$, n=6).

Comparison of the amounts of CAN formed in the skin following topical application of the 0.1% SPL nanomicelles showed no significant difference between the solution and hydrogel except in the upper dermis with infinite dose conditions (11.04 ± 3.71 *vs.* 6.39 ± 1.33 ng/cm^2, respectively; p<0.001). This was to be expected given the greater amounts of SPL found in the upper dermis after application of the 0.1% SPL nanomicellar hydrogel under infinite dose conditions.

Quantification of the receiver compartment showed no transdermal permeation through the skin after topical application for 12 h of the 0.1% SPL micellar formulations at finite dose, which mimics the real use conditions. However, application of 0.1% SPL micellar solution and hydrogel to porcine skin at infinite dose led to the permeation of 354.57 ± 79.18 and 443.98 ± 134.23 ng/cm^2, respectively. CAN was also detected in the receiver compartment after 12 h topical application of 0.1% SPL micellar solution and hydrogel, with permeation of 15.49 ± 3.52 and 20.24 ± 6.42 ng/cm^2, respectively.

3.4. Spironolactone follicular deposition

Fig. 4 shows typical skin biopsies obtained by punching out the pilosebaceous unit (PSU) and the PSU-free samples following topical application of the 0.1% SPL nanomicellar formulations.

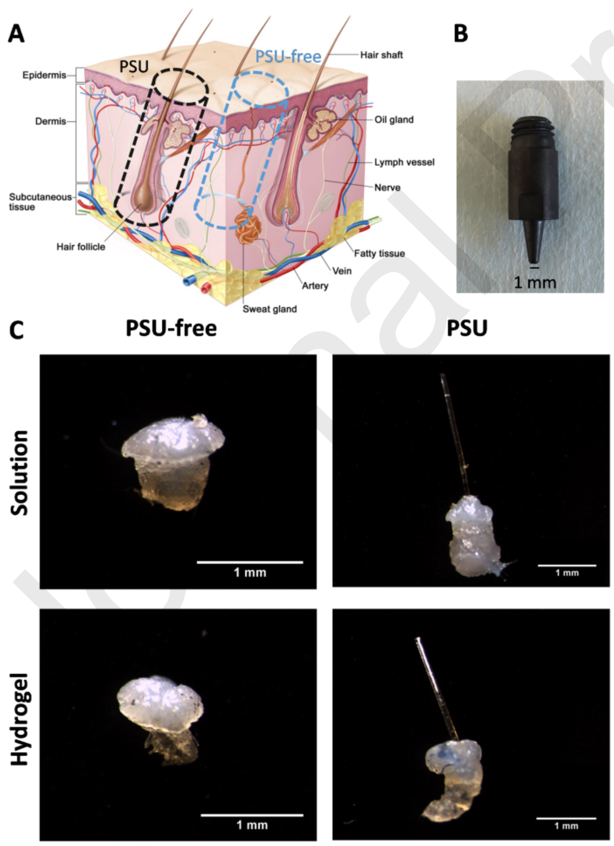

Fig. 4 (A) Schematic representation of a skin cross-section showing where the pilosebaceous unit (PSU) and the PSU-free skin biopsies were taken (used and adapted with permission from (Korotkov and Garcia, 2012) and ©2021 Terese Winslow LLC), (B) the punch used to obtain

the skin biopsies, and (C) typical skin biopsies obtained after punching out PSU-free and PSU-containing skin samples.

Comparison of the amounts of SPL deposited in the PSU-containing and PSU-free skin samples showed significantly higher amounts of SPL found in the former following topical application of both the 0.1% SPL nanomicellar solution and hydrogel under infinite and finite dose conditions (**Fig. 5**).

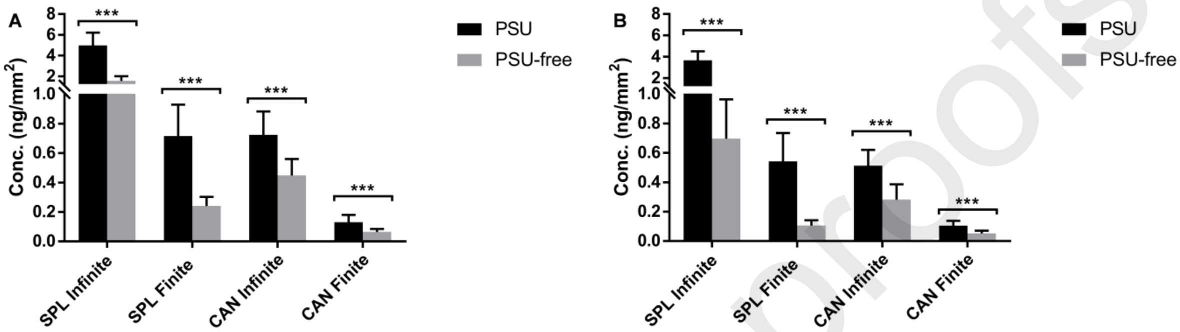

Fig. 5 Spironolactone (SPL) and canrenone (CAN) deposition in the pilosebaceous unit (PSU) and the PSU-free skin biopsies following topical application of (**A**) 0.1% SPL nanomicellar solution and (**B**) 0.1% SPL nanomicellar hydrogel in both infinite and finite dose conditions. (Mean ±SD ,*** $p<0.001$; n=15).

The amounts of SPL deposited in the PSU-containing skin samples were 3-fold higher than the PSU-free skin samples after topical application of the 0.1% SPL nanomicellar solution at both infinite (4.97 ± 1.20 *vs.* 1.56 ± 0.45 ng/mm^2, respectively; $p<0.001$) and finite (0.72 ± 0.21 *vs.* 0.24 ± 0.06 ng/mm^2, respectively; $p<0.001$) dose conditions. This difference was increased after topical application of the 0.1% SPL nanomicellar hydrogel – now PSU samples contained 5-fold more SPL at both infinite (3.67 ± 0.82 *vs.* 0.70 ± 0.26 ng/mm^2, respectively; $p<0.001$) and finite (0.54 ± 0.18 *vs.* 0.10 ± 0.03 ng/mm^2, respectively; $p<0.001$) dose conditions (**Fig. 5**).

The amounts of CAN found in the PSU-containing skin samples were 2-fold greater than those in the PSU-free samples after topical application of 0.1% SPL micellar solution at infinite (0.73 ± 0.15 *vs.* 0.45 ± 0.11 ng/mm^2, respectively; $p<0.001$) and finite (0.13 ± 0.05 *vs.* 0.06 ± 0.02 ng/mm^2, respectively; $p<0.001$) doses. Topical application of the 0.1% SPL micellar hydrogel also led to 2-fold greater amounts of CAN being present in the PSU skin samples compared to the PSU-free skin samples at infinite (0.51 ± 0.10 *vs.* 0.28 ± 0.10 ng/mm^2, respectively;

p<0.001) and finite (0.10 ± 0.03 *vs.* 0.05 ± 0.02 ng/mm^2, respectively; p<0.001) dose conditions (**Fig. 5**).

4. Discussion

4.1. Localization of the mineralocorticoid receptor in the skin

Despite extensive research, we could only find one study describing the localization of the MR in the skin (Kenouch et al., 1994). In contrast, many recent studies have reported on the emerging roles of the MR in skin physiology and in cutaneous wound healing. Given that the aim was to develop an SPL formulation to target the MR in the skin, it was clear that we needed to first identify where the target was located so as to better design the drug delivery system.

This is the first study demonstrating the presence and the localization of the MR in porcine skin using immunofluorescence labelling; Kenouch *et al.* assessed the presence of the MR in human skin using *in situ* hybridization and immunohistochemistry (Kenouch et al., 1994), and their findings were consistent with our results since they reported the localization of the MR in the hair follicle and the sweat glands. They also commented on the presence of the MR in the sebaceous glands and the epidermis, which was less obvious in our results. The presence of MR in the epithelial cells of the eccrine sweat glands is not surprising since MR and aldosterone regulate fluid secretion and electrolyte homeostasis through activation of the Na^{+}-K^{+}-ATPase during sudation (Kern et al., 1997; Sasano et al., 1992).

The immunofluorescence results confirmed that the MR was predominantly found in the PSU. This was extremely important since we have previously used qualitative and quantitative techniques to establish that mPEG-hexPLA micelles accumulate preferentially in the PSU following topical application to the skin: (i) qualitatively – visualization of skin samples using CLSM, following topical application of Nile Red-labelled mPEG-hexPLA micelles containing tacrolimus, showed a preferential accumulation of the NR-labelled copolymer around the hair follicle (Lapteva et al., 2014a), (ii) quantitatively – by comparing the amounts of the drug delivered to the PSU-containing *versus* PSU-free skin samples using UHPLC-MSMS analytical methods which showed a 2-fold higher delivery to the PSU-containing samples (Lapteva et al., 2015). These findings validated the strategy of using mPEG-hexPLA nanomicelles as carriers to deliver SPL to the skin.

4.2. SPL delivery to the epidermis and the upper dermis following topical application of the nanomicelles

The biodistribution study showed that the viscosity of the formulation did not affect the efficiency of SPL deposition in the epidermis. Nevertheless, the hydrogel was significantly more efficient ($p<0.001$) for delivery to the upper dermis under infinite dose and the solution was significantly more efficient ($p<0.05$) for delivery to the upper dermis under finite dose conditions. One possible explanation could be that under infinite dose conditions, the hydrogel increases the residence time of the SPL micellar formulation on the skin, acting as a reservoir, leading to a higher deposition over time compared to the micellar solution (which may leak or evaporate over time). In finite dose conditions, as the formulation amount applied is much lower, the reservoir effect provided by the hydrogel is less significant, and may have retarded the deposition of SPL into the epidermis compared to the solution given the higher viscosity.

Regardless of the delivery efficiency, both the solution and the hydrogel enabled the delivery of therapeutic amounts of SPL up to a skin depth of 400 μm and to the PSU-containing and PSU-free skin samples after application of both finite and infinite doses of 0.1% SPL micelles. Spironolactone IC_{50} is reported to be around 2 nM in the muscle (Chadwick et al., 2017; Garthwaite and McMahon, 2004; Sica, 2005); the biodistribution study showed that the nanomicelles could deliver spironolactone to the upper dermis in amounts ~150-fold higher than the IC_{50} with the micellar hydrogel and up to 250-fold higher with the micellar solution, under finite dose conditions.

Moreover, the active metabolite CAN also contributes to antagonism of the MR and was detected to a skin depth 400 μm and in the PSU. Interestingly, and unlike our findings following topical application of the 0.1% SPL nanomicelles to rabbit cornea *in vivo*, 7α-thiomethylspironolactone (TMSPL), another active metabolite was not detected in porcine skin *in vitro* following topical application of 0.1% SPL nanomicelles (Dahmana et al., 2018b). This may be due to interspecies differences (pig vs rabbit), to the experimental conditions, i.e. (*in vivo* vs *in vitro*), or to physiological differences such as enzyme expression (esterases, S-methyltransferases), between the cornea and the skin. It should be noted that in the *in vivo* study, 0.1% SPL nanomicelles were instilled up to 6 six times daily for 5 days to the rabbit eye; hence, TMSPL may be formed only after multiple dosing. Recent studies have reported that TMSPL is the main active metabolite of SPL in contrast to earlier work; this was due to the use of non-specific analytical methods that were unable to distinguish between CAN and other thiol-containing metabolites (Los et al., 1994). Metabolization of SPL occurs first via deacetylation catalysed by esterases forming the intermediate metabolite, 7α-thiospironolactone (TSPL), which undergoes S-methylation catalysed by thio-methyltranserase (TMT) forming 7α-thiomethylspironolactone (Keith et al., 1984). Some studies reported that canrenone is formed via sulfoxide elimination of the thioester S-oxide group from 7α-thiomethylspironolactone S-oxide via non-enzymatic pathway leading to removal of the sulfur moiety (Cashman and Pena, 1989).

Given that SPL was not detected in the receiver compartment after formulation application under finite dose conditions, i.e. the concentration was below the LOD of the UHPLC-ESI-MS method (5 ng/mL), systemic concentrations following application *in vivo* will be extremely low. Although transdermal permeation was observed with infinite dose conditions, this was still only 354.57 ± 79.18 and 443.98 ± 134.23 ng/cm^2, for the solution and hydrogel, respectively. Given that the hair follicle penetrates down to the subcutaneous tissue, it is possible that since the skin samples, with a thickness 800 µm, were prepared by slicing away the underlying tissue, this may have altered the integrity of the PSU by cutting the hair follicle resulting in the formation of a conduit communicating between the donor and the receiver compartments.

4.3. Targeted follicular delivery of SPL nanomicelles

0.1% SPL nanomicelles were shown to target the hair follicle preferentially with up to 5-fold higher amounts of SPL delivered to the PSU compared to the PSU-free skin biopsies. These findings are in accordance with our previous studies where topical application of mPEG-hexPLA nanomicelles containing retinoic acid showed a 2-fold higher delivery to the PSU compared to the PSU-free skin samples, and adapalene-containing TPGS based nanomicelles showed up to 4.5-fold higher delivery to the PSU compared to the PSU-free skin samples (Kandekar et al., 2017; Lapteva et al., 2015).

The solution delivered 1.3-fold higher amounts of SPL to the PSU compared to the hydrogel in both infinite (4.97 ± 1.20 *vs.* 3.67 ± 0.82 ng/mm^2, respectively; p=0.001) and finite (0.72 ± 0.21 *vs.* 0.54 ± 0.18 ng/mm^2, respectively; p=0.001) doses. This may be explained by the different rheological behaviour of the dosage forms with the solution having more facility to penetrate and flow through the follicular duct compared to the more viscous hydrogel. Nevertheless, both forms allowed the delivery of therapeutic amounts of SPL to the target site, i.e. the MR located in the hair follicle.

4.4. Beyond the mineralocorticoid receptor – other clinical targets for spironolactone in the pilosebaceous unit

Follicular delivery and the ability to administer drugs preferentially to the follicle has been the object of many studies, especially with the advent of nanotechnologies for topical drug delivery and has several potential benefits and therapeutic applications. First, in terms of site-specific drug delivery, in order to target PSU-associated disorders such as acne vulgaris, alopecia areata and hirsutism, thereby providing a higher therapeutic efficacy and minimizing the risk of side effects due to systemic exposure. Second, by providing a possible shunt penetration pathway to circumvent the stratum corneum barrier and improve drug bioavailability in the epidermis and dermis following topical application; the infundibular part of the hair follicle (the upper part) is more permeable to substances than the rest of the stratum corneum (Meidan et al., 2005; Patzelt and Lademann, 2013; Rancan and Vogt, 2014). Indeed, the hair follicle is an invagination and a continuation of the epidermis extending deep into the dermis, providing a larger contact area of the skin available for drug diffusion. Studies have reported that after topical application of particulate formulations, substances penetrate through the hair follicle orifice, accumulate in the follicular duct and form a reservoir that enables sustained release and continuous diffusion of substances to the follicular and the perifollicular cells and even reaching the viable skin strata by lateral diffusion (Hansen and Lehr, 2014; Meidan et al., 2005; Rancan and Vogt, 2014).

From a physiological perspective, the PSU is considered as the endocrine organ of the skin as it expresses the androgen, estrogen, progesterone, glucocorticoid and mineralocorticoid receptors and synthesizes various hormones. This makes it an interesting target for the treatment of numerous "hormone-dependent / hormone-related" skin and hair conditions (Chen and Zouboulis, 2009; Deplewski and Rosenfield, 2000; Reichrath, 2009; Zouboulis, 2000, 2009).

In addition to its antagonism of the MR, spironolactone is a potent antagonist of the androgen receptor (AR) which, as mentioned above, is also located in the PSU, mainly in the sebocytes of the sebaceous gland and the dermal papilla of the hair follicle (Choudhry et al., 1992). Androgens mediate sebocyte proliferation, sebum production and hair growth; their excess results in various skin and hair conditions such as acne vulgaris, seborrhoea, androgenic alopecia and hirsutism (Zouboulis et al., 2007).

In most patients suffering from androgen-related skin and hair conditions, the circulating androgen levels were found to be normal. The cutaneous hyperandrogenism characterizing these skin and hair diseases is reported to be due to *in situ* overexpression of 5α-reductase, which converts testosterone to the more potent 5α-dihydrotestosterone (5α-DHT) and the hyper-responsiveness of the AR. Hence, the importance of developing a local and site-specific drug delivery system for the treatment of these diseases for better efficacy and safety (Mercurio and Gogstetter, 2000). Acne is mostly due to excess of sebum production by the sebaceous glands through androgen stimulation, mainly by 5α-DHT. SPL, with its anti-androgenic activity, competitively inhibits 5α-DHT from binding to the AR thus decreasing sebum production. Several studies have reported the efficacy of the use of SPL to treat acne in patients (Afzali et al., 2012b; Berardesca et al., 1988; Kelidari et al., 2016; Lademann et al., 2008; Lademann et al., 2006; Lademann et al., 2007; Mercurio and Gogstetter, 2000).

Hirsutism is the presence of excessive hair growth affecting mostly women and is most often caused by increased production of androgens. Hence, oral SPL was used to treat hirsutism and significantly showed decreased hair growth (Brown et al., 2009; Burke and Cunliffe, 1985). Androgenic alopecia, characterized by hair loss and affects mostly men, is also due to excessive production of androgens. SPL was used to treat androgenic alopecia and results showed decreased androgen production within the sebaceous glands and blocking of the AR in dermal papillae (Adamopoulos et al., 1997; Burke and Cunliffe, 1985; Shamma and Aburahma, 2014).

In addition to these potential clinical applications, transfollicular delivery may be exploited to target the stem cells located in the bulge region of the hair follicle which could provide opportunities for the treatment of wound healing and inflammatory skin diseases (Hansen and Lehr, 2014; Meidan et al., 2005; Patzelt and Lademann, 2013).

Thus, in addition to the site-specific management of MR-mediated cutaneous wound healing, 0.1% SPL nanomicelles may be used for the treatment of multiple dermatological diseases associated with the PSU.

5. Conclusion

The successful development of 0.1% SPL nanomicellar formulations for topical application to the skin enabled the delivery of therapeutic amounts of spironolactone to the epidermis and the upper dermis. The results also confirmed the preferential delivery of SPL nanomicelles to the PSU, enabling the site-specific targeting of the mineralocorticoid receptor located, as we have demonstrated, in the hair follicle. Topical co-administration of 0.1% SPL nanomicelles could thereby offset glucocorticoid agonism of the mineralocorticoid receptor responsible for delayed cutaneous wound healing. This could be of considerable clinical relevance since patients would benefit from the anti-inflammatory effects of the glucocorticoids while spared the off-target glucocorticoid-induced side effects and with only a limited risk of SPL entry into the systemic circulation. Finally, given that SPL is also a potent anti-androgen, its targeted follicular delivery from the 0.1% SPL nanomicellar formulations may be of significant interest for other clinical applications such as androgen-mediated skin and hair diseases including acne vulgaris, androgenic alopecia and hirsutism.

Conflicts of interest

There are no conflicts to declare.

Acknowledgements

ND and YNK acknowledge financial support from the Swiss Commission for Technology and Innovation (CTI Project 19086.1 PFLS-LS) and Apidel SA (Geneva, Switzerland). YNK would like to thank the University of Geneva, the Fondation Ernst and Lucie Schmidheiny and the Société Académique de Genève for providing financial support to enable the acquisition of the Waters Xevo® TQ-MS detector. We would also like to thank Dr Christoph Bauer and Jérôme Bosset from the Bioimaging Center of the University of Geneva for their precious advice with TEM and CLSM.

References

Adamopoulos, D.A., Karamertzanis, M., Nicopoulou, S., Gregoriou, A., 1997. Beneficial effect of spironolactone on androgenic alopecia. Clin Endocrinol (Oxf) 47, 759-760.

Afzali, B.M., Yaghoobi, E., Yaghoobi, R., Bagherani, N., Dabbagh, M.A., 2012a. Comparison of the efficacy of 5% topical spironolactone gel and placebo in the treatment of mild and moderate acne vulgaris: a randomized controlled trial. Journal of Dermatological Treatment 23, 21-25.

Afzali, B.M., Yaghoobi, E., Yaghoobi, R., Bagherani, N., Dabbagh, M.A., 2012b. Comparison of the efficacy of 5% topical spironolactone gel and placebo in the treatment of mild and moderate acne vulgaris: a randomized controlled trial. J Dermatolog Treat 23, 21-25.

Berardesca, E., Gabba, P., Ucci, G., Borroni, G., Rabbiosi, G., 1988. Topical spironolactone inhibits dihydrotestosterone receptors in human sebaceous glands: an autoradiographic study in subjects with acne vulgaris. Int J Tissue React 10, 115-119.

Boix, J., Sevilla, L.M., Saez, Z., Carceller, E., Perez, P., 2016. Epidermal mineralocorticoid receptor plays beneficial and adverse effects in skin and mediates glucocorticoid responses. J Invest Dermatol 136, 2417-2426.

Brown, J., Farquhar, C., Lee, O., Toomath, R., Jepson, R.G., 2009. Spironolactone versus placebo or in combination with steroids for hirsutism and/or acne. Cochrane Database Syst Rev, CD000194.

Burke, B.M., Cunliffe, W.J., 1985. Oral spironolactone therapy for female patients with acne, hirsutism or androgenic alopecia. Br J Dermatol 112, 124-125.

Cashman, J.R., Pena, S., 1989. Canrenone formation via general-base-catalyzed elimination of 7 alpha-(methylthio)spironolactone S-oxide. Chem Res Toxicol 2, 109-113.

Chadwick, J.A., Hauck, J.S., Gomez-Sanchez, C.E., Gomez-Sanchez, E.P., Rafael-Fortney, J.A., 2017. Gene expression effects of glucocorticoid and mineralocorticoid receptor agonists and antagonists on normal human skeletal muscle. Physiol Genomics 49, 277-286.

Chen, W.C., Zouboulis, C.C., 2009. Hormones and the pilosebaceous unit. Dermatoendocrinol 1, 81-86.

Choudhry, R., Hodgins, M.B., Van der Kwast, T.H., Brinkmann, A.O., Boersma, W.J., 1992. Localization of androgen receptors in human skin by immunohistochemistry: implications for the hormonal regulation of hair growth, sebaceous glands and sweat glands. J Endocrinol 133, 467-475.

Dahmana, N., Gabriel, D., Gurny, R., Kalia, Y.N., 2018a. Development and validation of a fast and sensitive UHPLC-ESI-MS method for the simultaneous quantification of spironolactone and its metabolites in ocular tissues. Biomed Chromatogr, e4287.

Dahmana, N., Mugnier, T., Gabriel, D., Kaltsatos, V., Bertaim, T., Behar-Cohen, F., Gurny, R., Kalia, Y.N., 2018b. Topical Administration of Spironolactone-Loaded Nanomicelles Prevents Glucocorticoid-Induced Delayed Corneal Wound Healing in Rabbits. Mol Pharm 15, 1192-1202.

Deplewski, D., Rosenfield, R.L., 2000. Role of hormones in pilosebaceous unit development. Endocr Rev 21, 363-392.

Di Tommaso, C., Bourges, J.L., Valamanesh, F., Trubitsyn, G., Torriglia, A., Jeanny, J.C., Behar-Cohen, F., Gurny, R., Moller, M., 2012. Novel micelle carriers for cyclosporin A topical ocular delivery: in vivo cornea penetration, ocular distribution and efficacy studies. Eur J Pharm Biopharm 81, 257-264.

Farman, N., Maubec, E., Poeggeler, B., Klatte, J.E., Jaisser, F., Paus, R., 2010. The mineralocorticoid receptor as a novel player in skin biology: beyond the renal horizon? Exp Dermatol 19, 100-107.

Gabriel, D., Mugnier, T., Courthion, H., Kranidioti, K., Karagianni, N., Denis, M.C., Lapteva, M., Kalia, Y., Moller, M., Gurny, R., 2016. Improved topical delivery of tacrolimus: A novel composite hydrogel formulation for the treatment of psoriasis. J Control Release 242, 16-24.

Garthwaite, S.M., McMahon, E.G., 2004. The evolution of aldosterone antagonists. Mol Cell Endocrinol 217, 27-31.

Hansen, S., Lehr, C.M., 2014. Transfollicular delivery takes root: the future for vaccine design? Expert Rev Vaccines 13, 5-7.

Jaisser, F., Farman, N., 2016. Emerging Roles of the Mineralocorticoid Receptor in Pathology: Toward New Paradigms in Clinical Pharmacology. Pharmacological reviews 68, 49-75.

Kandekar, S.G., Del Rio-Sancho, S., Lapteva, M., Kalia, Y.N., 2017. Selective delivery of adapalene to the human hair follicle under finite dose conditions using polymeric micelle nanocarriers. Nanoscale 10, 1099-1110.

Keith, R.A., Jardine, I., Kerremans, A., Weinshilboum, R.M., 1984. Human erythrocyte membrane thiol methyltransferase. S-methylation of captopril, N-acetylcysteine, and 7 alpha-thio-spirolactone. Drug Metab Dispos 12, 717-724.

Kelidari, H.R., Saeedi, M., Hajheydari, Z., Akbari, J., Morteza-Semnani, K., Akhtari, J., Valizadeh, H., Asare-Addo, K., Nokhodchi, A., 2016. Spironolactone loaded nanostructured lipid carrier gel for effective treatment of mild and moderate acne vulgaris: A randomized, double-blind, prospective trial. Colloids and Surfaces B: Biointerfaces 146, 47-53.

Kenouch, S., Lombes, M., Delahaye, F., Eugene, E., Bonvalet, J.P., Farman, N., 1994. Human skin as target for aldosterone: coexpression of mineralocorticoid receptors and 11 beta-hydroxysteroid dehydrogenase. J Clin Endocrinol Metab 79, 1334-1341.

Kern, R.C., Foster, J.D., Pitovski, D.Z., 1997. Mineralocorticoid (type I) receptors in the olfactory mucosa of the mammal: studies with [3H]aldosterone and the anti-mineralocorticoid spironolactone. Chem Senses 22, 141-148.

Korotkov, K., Garcia, R., 2012. Computerized analysis of pigmented skin lesions: A review. Artificial Intelligence in Medicine 56, 69-90.

Lademann, J., Knorr, F., Richter, H., Blume-Peytavi, U., Vogt, A., Antoniou, C., Sterry, W., Patzelt, A., 2008. Hair follicles--an efficient storage and penetration pathway for topically applied substances. Summary of recent results obtained at the Center of Experimental and Applied Cutaneous Physiology, Charite -Universitatsmedizin Berlin, Germany. Skin Pharmacol Physiol 21, 150-155.

Lademann, J., Richter, H., Schaefer, U.F., Blume-Peytavi, U., Teichmann, A., Otberg, N., Sterry, W., 2006. Hair follicles - a long-term reservoir for drug delivery. Skin Pharmacol Physiol 19, 232-236.

Lademann, J., Richter, H., Teichmann, A., Otberg, N., Blume-Peytavi, U., Luengo, J., Weiss, B., Schaefer, U.F., Lehr, C.M., Wepf, R., Sterry, W., 2007. Nanoparticles--an efficient carrier for drug delivery into the hair follicles. Eur J Pharm Biopharm 66, 159-164.

Lapteva, M., Moller, M., Gurny, R., Kalia, Y.N., 2015. Self-assembled polymeric nanocarriers for the targeted delivery of retinoic acid to the hair follicle. Nanoscale 7, 18651-18662.

Lapteva, M., Mondon, K., Moller, M., Gurny, R., Kalia, Y.N., 2014a. Polymeric micelle nanocarriers for the cutaneous delivery of tacrolimus: a targeted approach for the treatment of psoriasis. Mol Pharm 11, 2989-3001.

Lapteva, M., Santer, V., Mondon, K., Patmanidis, I., Chiriano, G., Scapozza, L., Gurny, R., Moller, M., Kalia, Y.N., 2014b. Targeted cutaneous delivery of ciclosporin A using micellar nanocarriers and the possible role of inter-cluster regions as molecular transport pathways. J Control Release 196, 9-18.

Los, L.E., Pitzenberger, S.M., Ramjit, H.G., Coddington, A.B., Colby, H.D., 1994. Hepatic metabolism of spironolactone. Production of 3-hydroxy-thiomethyl metabolites. Drug Metab Dispos 22, 903-908.

Maubec, E., Laouenan, C., Deschamps, L., Nguyen, V.T., Scheer-Senyarich, I., Wackenheim-Jacobs, A.C., Steff, M., Duhamel, S., Tubiana, S., Brahimi, N., Leclerc-Mercier, S., Crickx, B., Perret, C., Aractingi, S., Escoubet, B., Duval, X., Arnaud, P., Jaisser, F., Mentre, F., Farman, N., 2015. Topical mineralocorticoid receptor blockade limits glucocorticoid-induced epidermal atrophy in human skin. J Invest Dermatol 135, 1781-1789.

Meidan, V.M., Bonner, M.C., Michniak, B.B., 2005. Transfollicular drug delivery--is it a reality? Int J Pharm 306, 1-14.

Mercurio, M.G., Gogstetter, D.S., 2000. Androgen physiology and the cutaneous pilosebaceous unit. J Gend Specif Med 3, 59-64.

Nguyen, V.T., Farman, N., Maubec, E., Nassar, D., Desposito, D., Waeckel, L., Aractingi, S., Jaisser, F., 2016. Re-Epithelialization of Pathological Cutaneous Wounds Is Improved by Local Mineralocorticoid Receptor Antagonism. The Journal of investigative dermatology 136, 2080-2089.

OECD, 2004. OECD Guideline for the testing of chemicals - Skin absorption: *in vitro* method. 428.

Patzelt, A., Lademann, J., 2013. Drug delivery to hair follicles. Expert Opin Drug Deliv 10, 787-797.

Rancan, F., Vogt, A., 2014. Getting under the skin: what is the potential of the transfollicular route in drug delivery? Ther Deliv 5, 875-877.

Reichrath, J., 2009. The skin is a fascinating endocrine organ. Dermatoendocrinol 1, 195-196.

Sasano, H., Fukushima, K., Sasaki, I., Matsuno, S., Nagura, H., Krozowski, Z.S., 1992. Immunolocalization of mineralocorticoid receptor in human kidney, pancreas, salivary, mammary and sweat glands: a light and electron microscopic immunohistochemical study. J Endocrinol 132, 305-310.

Schacke, H., Docke, W.D., Asadullah, K., 2002. Mechanisms involved in the side effects of glucocorticoids. Pharmacol Ther 96, 23-43.

Shamma, R.N., Aburahma, M.H., 2014. Follicular delivery of spironolactone via nanostructured lipid carriers for management of alopecia. Int J Nanomedicine 9, 5449-5460.

Sica, D.A., 2005. Pharmacokinetics and pharmacodynamics of mineralocorticoid blocking agents and their effects on potassium homeostasis. Heart Fail Rev 10, 23-29.

Trimaille, T., Mondon, K., Gurny, R., Moller, M., 2006. Novel polymeric micelles for hydrophobic drug delivery based on biodegradable poly(hexyl-substituted lactides). Int J Pharm 319, 147-154.

Werner, S., Grose, R., 2003. Regulation of wound healing by growth factors and cytokines. Physiol Rev 83, 835-870.

Zouboulis, C.C., 2000. Human skin: an independent peripheral endocrine organ. Horm Res 54, 230-242.

Zouboulis, C.C., 2009. The skin as an endocrine organ. Dermatoendocrinol 1, 250-252.

Zouboulis, C.C., Chen, W.C., Thornton, M.J., Qin, K., Rosenfield, R., 2007. Sexual Hormones in Human Skin. Horm Metab Res 39, 85-95.

Declaration of interests

☒ The authors declare that they have no known competing financial interests or personal relationships that could have appeared to influence the work reported in this paper.

☐The authors declare the following financial interests/personal relationships which may be considered as potential competing interests: